14th Australasian Fluid Mechanics Conference
Adelaide University, Adelaide, Australia
10-14 December 2001

Structures in a Round Homogeneous Jet at Low Reynolds Number

P.L. O'Neill, D. Honnery and J. Soria

Laboratory for Turbulence Research in Aerospace & Combustion
Department of Mechanical Engineering
Monash University, Melbourne, Victoria, 3800 AUSTRALIA

Abstract

The formation of structures in the shear layer of an unforced, incompressible, free, spatially evolving, round, homogeneous jet is investigated using flow visualisation and multigrid cross-correlation digital particle image velocimetry (MCCDPIV). It has been known for some time that the structures formed in such a jet can either be axisymmetric or helical, however the critical Reynolds number at which these structures occur and at the transition from one form to the other has not been conclusively resolved.

Introduction

Over the years there have been many experimental studies carried out on axisymmetric jets at high Reynolds numbers, as would occur in typical engineering applications. However, only few studies have investigated low Reynolds number axisymmetric jets. The low Reynolds number studies have investigated various aspects of the onset and growth of structures in the flow. Two distinct structures have been identified: axisymmetric and helical. Axisymmetric structures are characterised by axisymmetric swelling and contraction of the jet; the jet appears to pulsate. Helical structures are characterised by a rhythmic undulation or twisting of the jet. The onset of these structures and the transition between them is a fundamental theoretical problem, as well as being important in technological processes where one may wish to preserve the laminar nature of the jet for control purposes, or to induce turbulence for more vigorous transport.

A summary of some of the past experimental work in this area is presented in Table 1. The main experimental technique used in the tabulated studies was flow visualisation. As can be seen from the table, the results are incomplete and inconclusive. Various explanations have been put forward to explain the disparity in the results, for example:

1. The near field jet, being highly unstable, is susceptible to external disturbances such as noise and vibration. External disturbances are used in studies of forced jets to promote specific structures. In some experiments jets are driven by fans and pumps, whose operating frequencies could be enhancing and preempting the onset of a specific structure in the shear layer, making the results "rig-dependent". [3]

2. From theoretical studies of low Reynolds number axisymmetric jets it has been found that the assumed velocity profile will influence the critical Reynolds number where flow structures develop [6]. If the onset of a structure depends on the velocity profile of the jet then the shape of the nozzle or orifice is a relevant parameter in an experimental study. In particular, the boundary layer thickness, which would be different for a tube, a square-edged orifice or a knife-edge orifice, has been identified as an important criterion in the production of instabilities and promotion of the various structures [1].

3. The jets are studied in a confined space where recirculation may influence the development of instabilities and subsequent structure in unpredictable ways.

In this study, to avoid external disturbances as described in (1), the axisymmetric jet is generated by a piston in a 700-mm long perspex cylinder. This is a different experimental set-up from the more conventional pump or fan-driven jets, and avoids the background disturbances due to the pump-vane frequency and fan-blade frequency respectively.

To investigate the effect of orifice shape and velocity profile on the onset of instability as described in (2), various orifice plate geometries are used.

Finally, to minimise the effect of recirculation described in (3) the jet is discharged into a very large volume of fluid. Although it is impossible to avoid recirculation in a confined jet, a large tank reduces the incidence and intensity of these effects. Furthermore, we can use our equipment to investigate the differences between a confined and unconfined jet by a simple modification.

In this study, flow visualisation is used to examine the flow structures over a range of Reynolds number for the confined and unconfined jet, and multigrid cross-correlation digital particle image velocimetry (MCCDPIV) is used to determine the instantaneous two-dimensional velocity and out of plane vorticity.

Experiment

Apparatus

Figure 1 is a schematic diagram of the experimental apparatus used in this study. The piston diameter is 50 mm and it is made from precision machined stainless steel and has a PVC face. It is driven by a computer-controlled stepper motor directly coupled to a stainless steel lead screw. The orifice plate is affixed at the end of the perspex cylinder, flush with the false wall in the tank. The orifice diameter is 10 mm. The tank internal dimensions are 1000 mm x 500 mm x 500 mm. During experiments on the confined jet the tank and piston cylinder are sealed and filled with filtered water. For the experiments on the unconfined jet the cap on the overflow pipe is removed.

The maximum Reynolds number in the experiments is 1000. This corresponds to an orifice exit velocity of 100 mm/s, and a piston velocity of 4 mm/s. The acceleration period required for the stepper motor to reach this velocity is 8 μs, or equivalently 16 μm of piston movement.

For the flow visualisation experiments kiton red dye was used and for the MCCDPIV experiments the flow was seeded with nominally 11 μm diameter hollow glass spheres (Potters spherical, s.g. 1.1). Two pulsed laser sheets generated by two Nd:YAG lasers of wavelength 532 nm were used for illumination. These lasers deliver 6 ns pulses of up to 400 mJ. The lasers were collimated to a co-planar 2 mm thick

SOURCE	RELEVANT FINDING
Reynolds (1962) [7]	for $50 < Re < 250$ axisymmetric structures (later shown to be due to background disturbance) for $100 < Re < 250$ long wavelength sinuous undulations for $Re > 300$ confused breakup
Viilu (1962) [10]	transition from stable to unstable flow occurred between $10.5 < Re < 11.8$
Mattingly & Chang (1974) [5]	at $Re = 300$ axisymmetric structures close to nozzle outlet further downstream - axisymmetric structures present in half the experiments helical structures in the other half
Crow & Champagne (1971) [2]	increasing Re from 100 to 1000 found a continuous evolution from helical to axisymmetric structures

Table 1: Results from studies of low Reynolds number axisymmetric jets

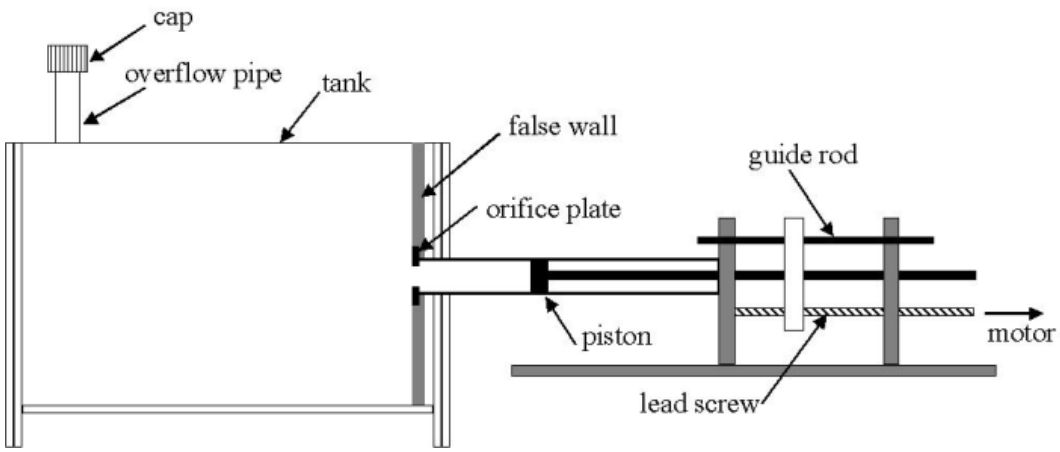

Figure 1: Schematic diagram showing the major components of the experimental rig. Diagram not to scale.

light sheet.

Image pairs consisting of two single-exposed images were recorded by a PCO Sensicam 12 bit cooled digital camera for both the flow visualisation and MCCDPIV experiments. The CCD array in this camera has over 1 million pixels (1280(H) x 1024(V)), and during a routine experiment can store 70 image pairs. For a Reynolds number of 1000, this would correspond to approximately 15 s of jet flow.

MCCDPIV Analysis Technique

The MCCDPIV software used to analyse the image pairs was developed by Soria ([8] and http://www-personal.monash.edu.au/∼julio), and uses an adaptive technique to increase the velocity dynamic range and reduce the bias and random errors in comparison to standard CCDPIV (eg [11]). The adaptive nature of the MCCDPIV technique takes advantage of the fact that the location of the interrogation windows in the two images do not necessarily have to coincide. By displacing the interrogation window in the second image by an amount approximately equal to the distance moved by the particles in Δt (the time separation between the two images) the measurable dynamic range of velocity is increased and the uncertainty of the measurement is reduced [9].

Results

The results presented here were obtained at a distance from $2D_0$ to $5D_0$ from the orifice outlet. At this time results have been obtained only for the sharp edged orifice shown in Figure 2.

Flow Visualisation Results

Flow visualisation was carried out over a range of Reynolds

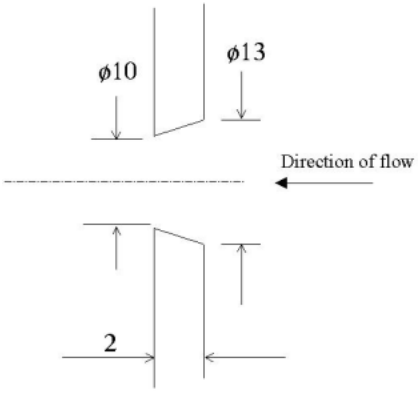

Figure 2: Profile of sharp edged orifice. All dimensions in mm. Diagram not drawn to scale

number from 100 to 1000 for both the confined and the unconfined jet to observe the onset of structures in the jet. At low Reynolds number – 300 or less for the confined jet and 250 or less for the unconfined jet – there was no discernible structure in the shear layer of the jet. An example of such a jet is shown in Figure 3. Between these low Reynolds number values and a Reynolds number of 450 for both the confined and unconfined jet, any structures in the jet were axisymmetric, but were small and poorly defined and interspersed with regions where there were no structures present. For the case of a confined jet with a Reynolds number of 500 both helical and axisymmetric structures were observed, and examples of both are shown in Figure 4. For high Reynolds number – 600 and above for the confined jet and 500 and above for the unconfined jet – well defined axisymmetric structures occurred.

JET CHARACTERISTIC	Re FOR CONFINED JET	Re FOR UNCONFINED JET
No structures in shear layer	300 and less	250 and less
small, poorly defined axisymmetric structures interspersed with regions with no structures	between 350 and 450	between 300 and 450
Both axisymmetric and helical structures present	500	not observed
Well defined axisymmetric structures only	between 600 and 1000	between 500 and 1000

Table 2: Summary of results from flow visualisation studies

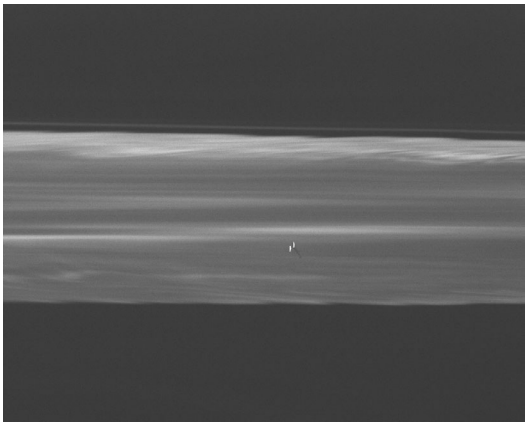

Figure 3: An example of the jet shape with no discernible structure in the shear layer. The Reynolds number is 250 and the jet is unconfined. Flow is from right to left.

These results are summarised in Table 2.

MCCDPIV Results

MCCDPIV was carried out over a range of Reynolds number for both the confined and unconfined jet. For the unconfined jet at a Reynolds number of 900 a typical velocity field together with a typical flow visualisation image is shown in Figure 5, while typical results for a Reynolds number of 600 are shown in Figure 6. The velocity fields presented have been filtered using a χ^2_{13} interpolation [4]. This removes noise and replaces data that has been identified as invalid. In all cases less than 5% of the data in the velocity field was identified as invalid prior to filtering.

From the flow visualisation images in Figures 5 and 6 it appears that in both situations the patterns of disturbance are axisymmetric, however while the velocity vector field for the $Re = 900$ case shows definite exchanges in momentum across the shear layer that would enhance these structures, for the $Re = 600$ case there is little evidence of exchange of momentum. The differences in the two velocity fields is further illustrated by the velocity profiles shown in Figure 7. These show the change in the z-direction centre line velocity along the jet. The data was extracted from the PIV fields shown in Figures 5 and 6. From the centre-line velocity plot for the jet at a Reynolds number of 900 it appears that the jet velocity increases through the contraction created by two concurrent axisymmetric structures and then slows down through the expansion. In comparison, the centre-line velocity for a Reynolds number of 600 changes only slightly with distance from the orifice.

Conclusions

From the flow visualisation results we observed a transition with increasing Reynolds number from a predominantly uniform jet with no structures evident in the shear layer to a jet with well defined axisymmetric structures apparent. This was observed for both the confined and unconfined jet. In addition, we observed an unstable jet structure for the confined jet at a Reynolds number of 500, where both helical and axisymmetric structures were apparent. No unstable transition from helical to axisymmetric structure was observed for the unconfined jet at any of the Reynolds numbers investigated.

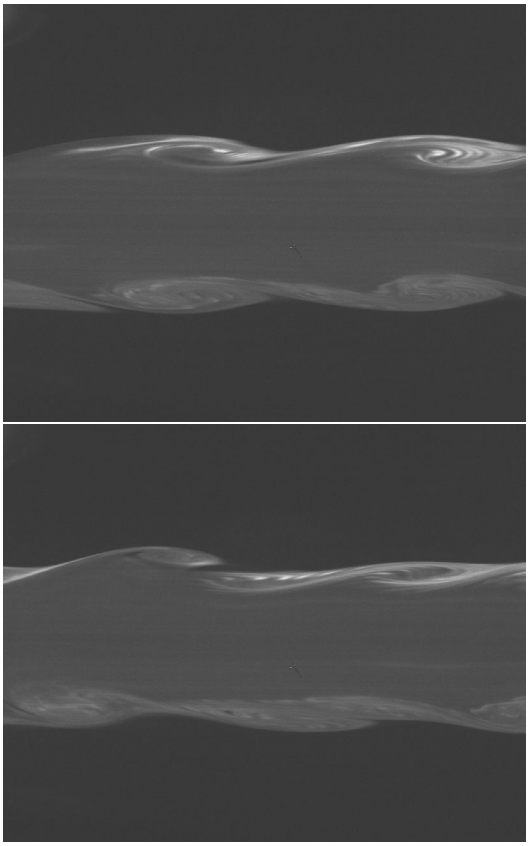

Figure 4: Flow visualisation images for the confined jet at a Reynolds number of 500. The top image shows axisymmetric structures, the bottom image shows helical structures. The time between the two images is approximately 0.25s. Flow is from right to left.

The flow visualisation results for the unconfined jet showed axisymmetric structures for the two Reynolds numbers of 900 and 600. However, the MCCDPIV results indicate that the mechanics associated with the production and maintenance of these structures appear to be quite different for the two conditions.

This work is part of an ongoing investigation into structures in low Reynolds number axisymmetric jets. In further work we will be investigating the effect of inducing turbulence behind the orifice plate and different orifice plate geometries on the development of the flow structures.

Acknowledgements

This work is supported by the Monash University ERG

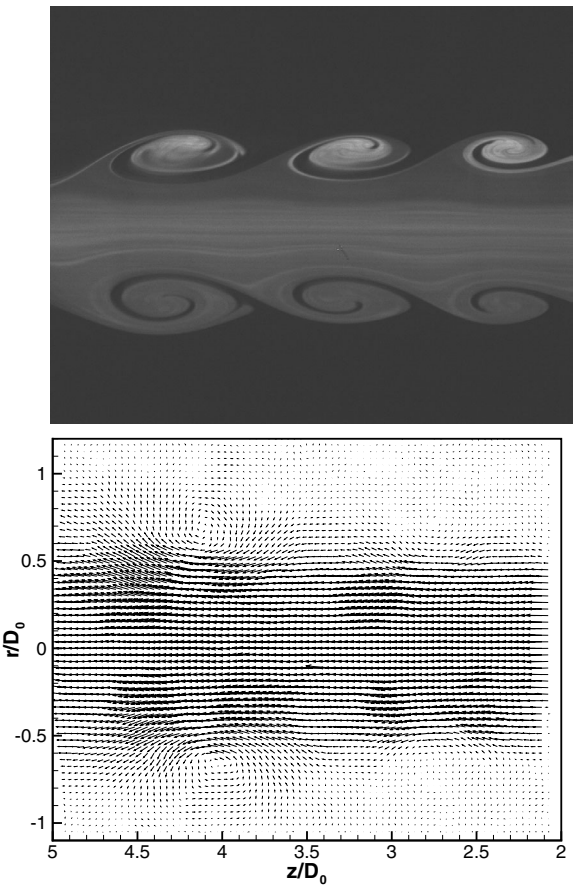

Figure 5: Typical flow visualisation image and velocity field for the unconfined jet at a Reynolds number of 900. Flow is from right to left

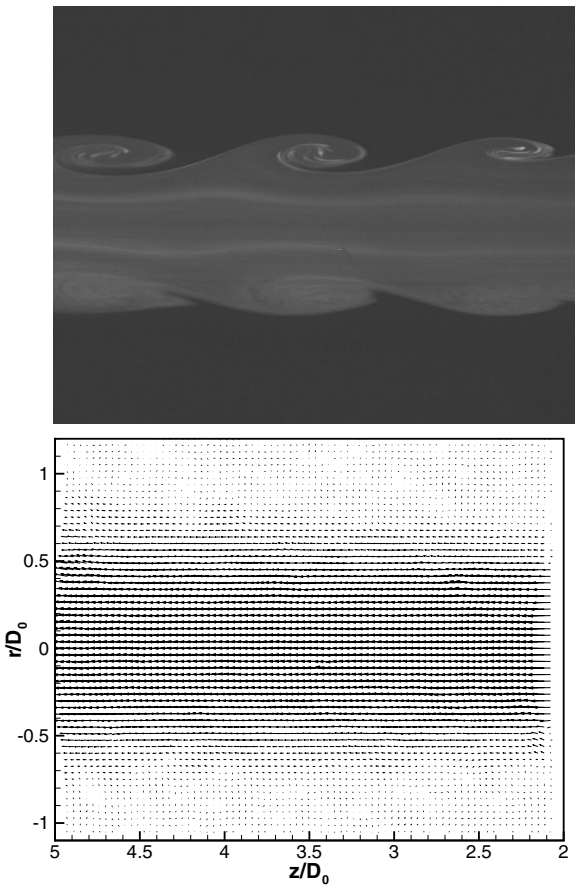

Figure 6: Typical flow visualisation image and velocity field for the unconfined jet at a Reynolds number of 600. Flow is from right to left.

scheme.

References

[1] H.A. Becker and T.A. Massaro, Vortex evolution in a round jet, *J. Fluid Mechanics*, **31**:435-448 (1968)

[2] S.C. Crow and F.H. Champagne, Orderly structure in jet turbulence, *Journal of Fluid Mechanics*, **43**:547-591 (1971)

[3] I. Danaila, J. Dušek, F. Anselmet, Coherent structures in a round, spatially evolving, unforced, homogeneous jet at low Reynolds numbers, *Physics of Fluids*, **9**:3323-3342 (1997)

[4] A. Fouras and J. Soria, Accuracy of out-of-plane vorticity measurements derived from in-plane velocity field data, *Experiments in Fluids*, **25**:409-430 (1998)

[5] G.E. Mattingly and C.C. Chang, Unstable waves on an axisymmetric jet column. *Journal of Fluid Mechanics*, **65**:541 (1974)

[6] Philip J. Morris, The spatial viscous instability of axisymmetric jets, *Journal of Fluid Mechanics*, **77**:511-529 (1976)

[7] A.J. Reynolds, Observations of a liquid-into-liquid jet, *Journal of Fluid Mechanics*, **14**:552-556 (1962)

[8] J. Soria, An adaptive cross-correlation digital PIV technique for unsteady flow investigations, *First Australian Conference on Laser Diagnostics in Fluid Mechanics and Combustion*, 29-45 (1996)

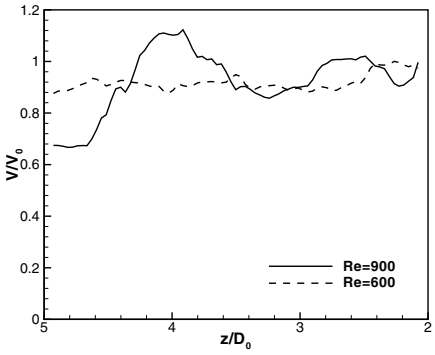

Figure 7: Normalised Z-direction centre line velocity for Reynolds numbers of 900 and 600. These plots were derived from the PIV fields shown in Figures 5 and 6

[9] J. Soria, Multigrid approach to cross-correlation digital PIV and HPIV analysis, *13th Australasian Fluid Mechanics Conference*, Monash University, Melbourne, 381-384 (1998)

[10] A. Viilu, An experimental determination of the minimum Reynolds number for instability in a free jet, *Journal of Applied Mechanics*, **29**:506 (1962)

[11] C.E. Willert and M. Gharib, Digital particle image velocimetry, *Experiments in Fluids*, **10**:181-193 (1991)